Comparison of Kinetic and Diffusional Models for Solid-Gas Reactions

M. ISHIDA and C. Y. WEN

West Virginia University, Morgantown, West Virginia

A comparison of the kinetic and diffusional models for solid-gas reactions occurring in a spherical particle is presented. The similarities and differences of the unreacted-core shrinking model and the homogeneous model are examined in light of the rate-controlling factors. In view of the similarity of the two models, it is shown that erroneous conclusions in regard to the mechanism and the activation energies may be drawn from an analysis of the experimental data. A more versatile model is presented in order to augment the two models so that wider varieties of solid-gas reaction systems may be treated. The concept of effectiveness factors in solid-gas reactions is introduced, and the influence of diffusion is ascertained.

Among the numerous important solid-gas reactions in the chemical and metallurgical industries, a few examples of those in which the solid does not appreciably change in size during the reaction are the reduction of metallic oxides, the roasting of ores, the nitrogenation of calcium carbide to produce cyanamide, the regeneration of carbon-deposited catalysts, etc. In a great majority of instances, the analysis of these solid-gas reactions has been based on the unreacted-core shrinking model as shown by Yagi

Masaru Ishida is with the Tokyo Institute of Technology, Tokyo, Japan.

and Kunii (7). This model is acceptable because the porosity of the unreacted solid is usually very small, meaning the solid is practically impervious to the gaseous reactants, and the reaction will occur at the surface of the solid or at the interface between the unreacted solid and the porous product layer. This model is also applicable when the chemical reaction rate is very rapid and the diffusion of gases is sufficiently slow. The zone of reaction in such a case will be narrowly confined to the interface between the unreacted solid and the product. On the other hand, if the solid contains enough voidage so that the gaseous reactant can diffuse freely into the interior of the solid, the unreacted-core shrinking model becomes no longer applicable. In such cases, the reactions between gas and solid may be viewed as occurring homogeneously throughout the solid to produce a gradual variation in solid reactant concentration in all parts of the particle. Therefore, another model, which we shall call the *homogeneous model,* is needed for the analysis of porous solid-gas reactions. Here, the solid may be considered as an ensemble of small lumps of reactant distributed uniformly throughout the solid phase. The effective diffusivities of gaseous components through the solid are considered large and are invariant during the reaction. Weisz and Goodwin (6) observed that in the combustion of carbonaceous deposits within the porous catalytic particles, at low temperature (450°C.) when chemical reaction is controlling, the carbon burn-off is uniform throughout the particle. Reactions occurring in ion-exchange resins can also be treated based on the homogeneous model.

Because of the mathematical difficulty, the homogeneous model has not been applied to solid-gas reactions except for some special cases. Ausman and Watson (1), using a pseudo steady state approximation for gas concentration distribution and a first-order reaction with respect to the gaseous reactant, obtained a general solution for a solid-gas reaction in a spherical particle based on the homogeneous model.

In actuality, however, solid-gas reactions cannot be completely described either by the unreacted-core shrinking model or by the homogeneous model. The majority of cases belonging to this class of solid-gas reactions are probably an intermediate of these two models. Therefore, it seems worthwhile to examine and clarify the relation of these models and to provide a possibility of developing a more versatile model applicable under a wide variety of conditions.

In the following discussion, we shall consider a more versatile model for solid-gas reactions which displays an intermediate of the unreacted-core shrinking model and the homogeneous model. In this connection, an analytical solution of this model will be obtained, and a comparison and an examination of the various models will be presented. In addition, the concept of the effectiveness factors developed in catalytic reactions will be extended to solid-gas reactions based on these models. The effects of the diffusion into the solid and across the gas film around the particle on these effectiveness factors will be shown.

A MODEL FOR SOLID-GAS REACTIONS

Let us consider a class of solid-gas reactions represented by

$$aA(g) + S(s) \rightarrow \text{products}$$

A material balance for gaseous reactant A and solid reactant S can be written as

$$\epsilon \frac{\partial C_A}{\partial t} = \nabla \cdot (D_{eA} \nabla C_A) - r_A \qquad (1)$$

$$\frac{\partial C_S}{\partial t} = -r_S \qquad (2)$$

where r_A and r_S are stoichiometrically related by $r_A = ar_S$, and are the rates of reaction for gas component A and for solid reactant S, respectively. The boundary conditions are

$$\left.\begin{aligned} D_{eA} \nabla C_A &= k_{mA}(C_{Ao} - C_A) && \text{at the solid surface} \\ \nabla C_A &= 0 && \text{at the center} \end{aligned}\right\} \qquad (3)$$

$$C_S = C_{So} \qquad \text{at } t = 0 \qquad (4)$$

A solution of the above equations for a spherical particle is given below under the following assumptions:

1. Pseudo steady state approximation for gas A is valid, or $\epsilon \dfrac{\partial C_A}{\partial t} = 0$. The pseudo steady state approximation has been shown to be valid for most solid-gas reactions.
2. The rate of reaction is independent of the solid reactant concentration but is first order with respect to the gaseous reactant A. Thus, $r_A = ak_v C_{So}(C_A - C_A^*)$.

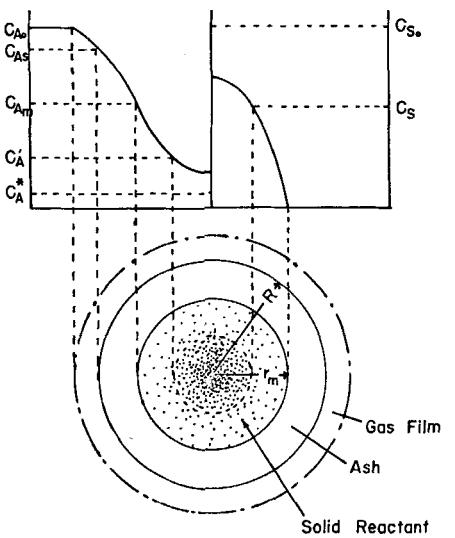

Fig. 1. Schematic diagram of concentration profile in the second stage.

Since the reaction is faster near the surface than in the interior of the particle, after a certain time the solid reactant near the surface will be completely exhausted forming an inert product layer (ash layer) as illustrated in Figure 1. We shall designate the period of reaction prior to the formation of the ash layer as the first stage, and the period following the ash layer formation as the second stage. For convenience, we shall use C'_A and D'_{eA} to denote the concentration and the effective diffusivity, respectively, of gas A in the solid during the first stage of the reaction and in the reaction zone during the second stage of the reaction. We shall use C_A and D_{eA} to denote the concentration and the effective diffusivity of gas A in the product ash layer during the second stage of reaction. We shall assume that D'_{eA} and D_{eA} are constant throughout the reaction.

The First Stage Reaction

A schematic diagram of the reacting particle during the first stage is shown in Figure 2. The material balance and the boundary conditions given in Equations (1), (2), and (3) now become

$$0 = D'_{eA}\left(\frac{d^2C'_A}{dr^2} + \frac{2}{r}\frac{dC'_A}{dr}\right) - ak_vC_{So}(C'_A - C_A^*) \tag{5}$$

$$\frac{\partial C_S}{\partial t} = -k_vC_{So}(C'_A - C_A^*) \tag{6}$$

$$\left.\begin{aligned} D'_{eA}\frac{dC'_A}{dr} &= k_{mA}(C_{Ao} - C'_A) \quad \text{at } r = R \\ \frac{dC'_A}{dr} &= 0 \quad \text{at } r = 0 \end{aligned}\right\} \tag{7}$$

The concentration profile of gas A in the particle can be obtained as

$$\frac{C'_A - C_A^*}{C_{Ao} - C_A^*} = \frac{1}{\theta_{vc}}\frac{\sinh(\phi'_v\xi)}{\xi\sinh\phi'_v} \tag{8}$$

where

$$\xi = \frac{r}{R},\quad \phi'_v = R\sqrt{\frac{ak_vC_{So}}{D'_{eA}}}$$

$$\theta_{vc} = 1 + \frac{1}{N'_{Sh}}(\phi'_v\coth\phi'_v - 1) \text{ and } N'_{Sh} = \frac{k_{mA}R}{D'_{eA}}$$

In Figure 3, the effect of the variation of ϕ'_v on the concentration profile of reactant gas A is shown for $N'_{Sh} = \infty$. For ϕ'_v larger than 50, the rate of chemical reaction becomes much faster than the diffusion through the solid, and, consequently, the reaction takes place before gas A can diffuse into the interior of the particle. The variation in the solid reactant concentration can be found from

$$C_S = C_{So} - \int_0^t k_vC_{So}(C'_A - C_A^*)\,dt$$

as

$$\frac{C_S}{C_{So}} = 1 - \frac{\sinh(\phi'_v\,\xi)}{\xi\sinh\phi'_v}\frac{\theta_v}{\theta_{vc}} \tag{9}$$

where θ_v, the dimensionless reaction time, is given by

$$\theta_v = k_v(C_{Ao} - C_A^*)\,t$$

The fractional conversion of solid reactant X is found from

$$X = 1 - \left[\int_0^R 4\pi r^2C_S dr \Big/ \int_0^R 4\pi r^2C_{So}dr\right]$$

as

$$X = \frac{3}{(\phi'_v)^2}(\phi'_v\coth\phi'_v - 1)\cdot\frac{\theta_v}{\theta_{vc}} \tag{10}$$

The rate of reaction per particle M_S = is found from $aM_S = M_A = 4\pi R^2k_{mA}(C_{Ao} - C_{AS})$ as

$$aM_S = M_A = \frac{4\pi RC_{Ao}D'_{eA}}{\theta_{vc}}(\phi'_v\coth\phi'_v - 1) \tag{11}$$

The length of time for the first stage reaction to last is obtained from Equation (9) by letting $\xi = 1$ and $C_S = 0$:

$$\theta_v = \theta_{vc} \tag{12}$$

As is evident from Equations (8) and (11), the concentration profile of gas component A and the rate of reaction per single particle are independent of time. Therefore, θ_{vc} can be regarded as the length of time (dimensionless) for the duration of the constant rate period. If the resistance to the gas film diffusion around the particle is negligibly small, that is, $N'_{Sh} = \infty$, then θ_{vc} becomes unity.

The solid reactant concentration distribution and the conversion at the end of the first stage can be found from Equations (9) and (10):

$$\frac{C_S}{C_{So}} = 1 - \frac{\sinh(\phi'_v\,\xi)}{\xi\sinh\phi'_v} \tag{13}$$

$$X = \frac{3}{(\phi'_v)^2}(\phi'_v\coth\phi'_v - 1) \tag{14}$$

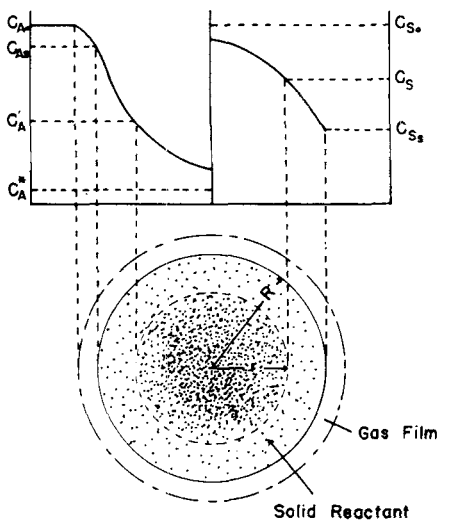

Fig. 2. Schematic diagram for concentration profile in the first stage.

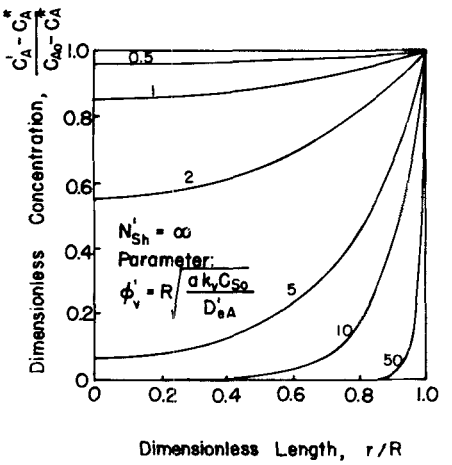

Fig. 3. Influence of parameter ϕ'_v on concentration profile of component A.

The Second Stage Reaction

As the reaction progresses, as shown in Figure 1, two zones appear: an outer zone in which the solid reactant is completely exhausted (the diffusion zone), and an inner zone where the reaction still takes place (the reaction zone). The material balance equations, the boundary conditions, and the initial conditions for the second stage reaction are shown in the following table.

Inner core (reaction zone)

$$0 = D'_{eA}\left(\frac{d^2C'_A}{dr^2} + \frac{2}{r}\frac{dC'_A}{dr}\right) - ak_vC_{So}\,(C'_A - C_A^*) \qquad (15)$$

$$\frac{\partial C_s}{\partial t} = -k_vC_{So}\,(C'_A - C_A^*) \qquad (16)$$

$$\frac{dC'_A}{dr} = 0 \qquad \text{at } r = 0 \qquad (17)$$

Outer layer (diffusion zone)

$$0 = D_{eA}\left(\frac{d^2C_A}{dr^2} + \frac{2}{r}\frac{dC_A}{dr}\right) \qquad (18)$$

$$C_S = 0 \qquad (19)$$

$$D_{eA}\frac{dC_A}{dr} = k_{mA}\,(C_{Ao} - C_A) \text{ at } r = R \qquad (20)$$

$$C'_A = C_A \qquad \text{at } r = r_m$$

$$D'_{eA}\frac{dC'_A}{dr} = D_{eA}\frac{dC_A}{dr} \qquad (21)$$

$$C_S = C_{So}\left[1 - \frac{\sinh(\phi'_v\,\xi)}{\xi\sinh\phi'_v}\right] \text{ at } t = t_c = \frac{\theta_{vc}}{k_v\,(C_{Ao} - C_A^*)} \text{ and } r_m = R \qquad (22)$$

The concentration distribution of gas A can be obtained from Equations (15), (17), (18), and (20) as

$$\frac{C'_A - C_A^*}{C_{Ao} - C_A^*} = \frac{C_{Am} - C_A^*}{C_{Ao} - C_A^*}\,\frac{\xi_m\sinh(\phi'_v\,\xi)}{\xi\sinh(\phi'_v\,\xi_m)} \qquad \text{for } 0 \leq r \leq r_m \qquad (23)$$

and

$$\frac{C_A - C_A^*}{C_{Ao} - C_A^*} = \frac{C_{Am} - C_A^*}{C_{Ao} - C_A^*}\cdot\frac{\xi_m}{\xi}\cdot\frac{1 - \xi + \xi/N_{Sh}}{1 - \xi_m + \xi_m/N_{Sh}} + \frac{1 - \xi_m/\xi}{1 - \xi_m + \xi_m/N_{Sh}} \qquad \text{for } r_m \leq r \leq R \qquad (24)$$

where $N_{Sh} = \dfrac{k_{mA}R}{D_{eA}}$, $\xi_m = \dfrac{r_m}{R}$, and C_{Am} is the concentration of gas A at the boundary of the two zones, or at $r = r_m$, and is obtained from Equation (21) as

$$\frac{C_{Am} - C_A^*}{C_{Ao} - C_A^*} = \frac{1}{1 + \dfrac{D'_{eA}}{D_{eA}}\left(1 - \xi_m + \dfrac{\xi_m}{N_{Sh}}\right)\,[\phi'_v\,\xi_m\,\coth(\phi'_v\xi) - 1]} \qquad (25)$$

In Figure 4, the variation of C_{Am} is shown as a function of ϕ_v $(= \phi'_v)$ when $N_{Sh} = \infty$ and $D_{eA} = D'_{eA}$. As the values of ϕ_v become larger, $C_{Am} - C_A^*$ is seen to approach zero.

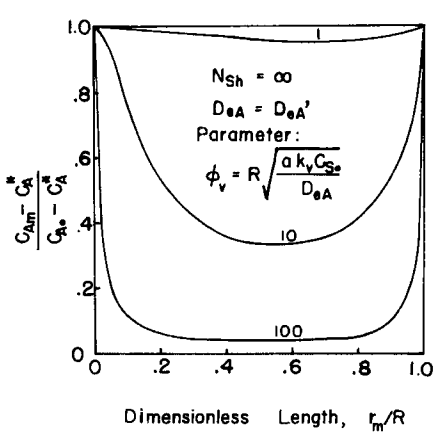

Fig. 4. Influence of ϕ_v on C_{Am}, the concentration of component A at the boundary.

This corresponds to the condition of the fast chemical reaction and the slow diffusion through solid, with the solid diffusion being the rate controlling factor. The variation in solid reactant concentration can be found from

$$C_S = (C_S)_{t_c} - \int_{t_c}^{t} k_vC_{So}(C'_A - C_A^*)\,dt$$

as

$$\frac{C_S}{C_{So}} = 1 - \frac{\sinh(\phi'_v\,\xi)}{\xi\sinh\phi'_v} - \frac{\sinh(\phi'_v\,\xi)}{\xi}\int_{\theta_{vc}}^{\theta_v}\frac{[\xi_m/\sinh(\phi'_v\,\xi_m)]\,d\theta_v}{1 + \dfrac{D'_{eA}}{D_{eA}}\left[1 - \xi_m + \dfrac{\xi_m}{N_{Sh}}\right]\,[\phi'_v\,\xi_m\coth(\phi'_v\,\xi_m) - 1]} \qquad (26)$$

The integration in Equation (26) requires the relation between θ_v and ξ_m. This can be found as follows. Differentiating Equation (26) with respect to θ_v at $\xi = \xi_m$ and $C_S = 0$, we obtain

$$\frac{d\theta_v}{d\xi_m} = -\frac{1}{\xi_m}\,[\phi'_v\,\xi_m\coth(\phi'_v\,\xi_m) - 1]\left[1 + \frac{D'_{eA}}{D_{eA}}\,(1 - \xi_m + \xi_m/N_{Sh})\cdot\{\phi'_v\,\xi_m\coth(\phi'_v\,\xi_m) - 1\}\right] \qquad (27)$$

Thus, the time required for the ash layer to reach r_m is obtained as

$$\theta_v = \theta_{vc} + \int_1^{\xi_m}\frac{d\theta_v}{d\xi_m}\,d\xi_m$$

Ausman and Watson (*1*) used the graphical method to obtain the above integration for $D_{eA} = D'_{eA}$. However, an analytical solution can be obtained as follows:

$$\theta_v = 1 + \left(1 - \frac{D'_{eA}}{D_{eA}}\right)\ln\frac{\xi_m\sinh\phi'_v}{\sinh(\phi'_v\,\xi_m)} + \frac{\phi_v^2}{6}(1 - \xi_m)^2\,(1 + 2\,\xi_m) + \frac{D'_{eA}}{D_{eA}}\,(1 - \xi_m)\,[\phi'_v\,\xi_m\coth(\phi'_v\,\xi_m) - 1] + \frac{1}{N_{Sh}}\cdot\frac{\phi_v^2}{3}\,(1 - \xi_m^3) + \frac{\xi_m}{N'_{Sh}}\,[\phi'_v\,\xi_m\coth(\phi'_v\,\xi_m) - 1] \qquad (28)$$

The time required for the reaction to complete both the first stage and the second stage, θ_v^*, can be found from

the above equation by letting $\xi_m = 0$ as

$$\theta_v^* = 1 + \frac{\phi_v^2}{6}\left(1 + \frac{2}{N_{Sh}}\right) + \left(1 - \frac{D'_{eA}}{D_{eA}}\right)\ln\frac{\sinh\phi'_v}{\phi'_v} \tag{29}$$

When we substitute Equation (28) into Equation (26), the concentration distribution for solid reactant is obtained as

$$\frac{C_S}{C_{So}} = 1 - \frac{\xi_m \sinh(\phi'_v\xi)}{\xi \sinh(\phi'_v\xi_m)} \tag{30}$$

and the solid reactant conversion is

$$X = 1 - \xi_m^3 + \frac{3\xi_m}{(\phi'_v)^2}[\phi'_v\xi_m\coth(\phi'_v\xi_m) - 1] \tag{31}$$

Equations (30) and (31) are the same as those obtained by Ausman and Watson (*1*).

Thus, we have completed the derivation of a model for a solid-gas reaction in a spherical particle. Next, we shall introduce the effectiveness factor η_v for this reaction so that the effect of diffusion can be more conveniently examined. Accordingly, the effectiveness factor η_v for solid-gas reaction is defined as

$$\eta_v = \frac{\text{actual reaction rate}}{\text{reaction rate obtainable when the gas concentration and temperature existing in the interior of the particle are the same as those existing in the bulk gas phase}}$$

Unlike the effectiveness factor used in catalytic reactions, which is based on the gas concentration and temperature at the surface of the catalysts, the effectiveness factor for solid-gas reaction is based on the concentration and temperature in the bulk gas phase which do not change during the reaction. Hence

$$\eta_v = \frac{\int k_v C_{So}(C'_A - C_A^*)dV}{\int k_v C_{So}(C_{Ao} - C_A^*)dV} \tag{32}$$

and is given as
The first stage:

$$\eta_v = \frac{3}{(\phi'_v)^2}[\phi'_v\coth\phi'_v - 1]\cdot\frac{1}{\theta_{vc}} \tag{33}$$

The second stage:

$$\eta_v = \frac{3}{(\phi'_v\xi_m)^2}\cdot\frac{\phi'_v\xi_m\coth(\phi'_v\xi_m) - 1}{1 + \frac{D'_{eA}}{D_{eA}}[1 - \xi_m + \xi_m/N_{Sh}][\phi'_v\xi_m\coth(\phi'_v\xi_m) - 1]} \tag{34}$$

The effectiveness factor as given in Equations (33) and (34) is equivalent to the ratio of the chemical reaction resistance to the total resistance consisting of the diffusional resistance and the chemical reaction resistance.

THE HOMOGENEOUS MODEL ($D_{eA} = D'_{eA}$)

If we let $D_{eA} = D'_{eA}$ in the model discussed in the previous section, we obtain the homogeneous model. Figure 5 shows the relation between the reaction time and the solid reactant conversion, for various values of ϕ_v $(= \phi'_v)$ in the case where the gas-film resistance is negligibly small, that is, $N_{Sh} = \infty$. As ϕ_v is increased, the diffusion of gas A through the solid becomes the rate-controlling factor, and the lines converge into one line. Under this condition, Equations (23), (24), (28), and (31) are reduced to

$$C_A = C_A^* \quad \text{for} \quad 0 \le r \le r_m$$

$$\frac{C_A - C_A^*}{C_{Ao} - C_A^*} = \frac{1 - \xi_m/\xi}{1 - \xi_m + \xi_m/N_{Sh}} \quad \text{for} \quad r_m \le r \le R$$

$$X = 1 - \xi_m^3$$

and

$$\frac{\theta_v}{\theta_v^*} = 1 - 3(1-X)^{2/3} + 2(1-X)$$

Also from Equation (29), $\theta_v^* \propto R^2$.

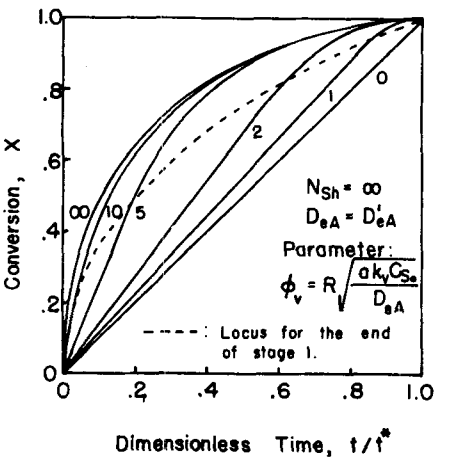

Fig. 5. Fractional conversion of solid reactant as a function of dimensionless time for homogeneous model (sphere).

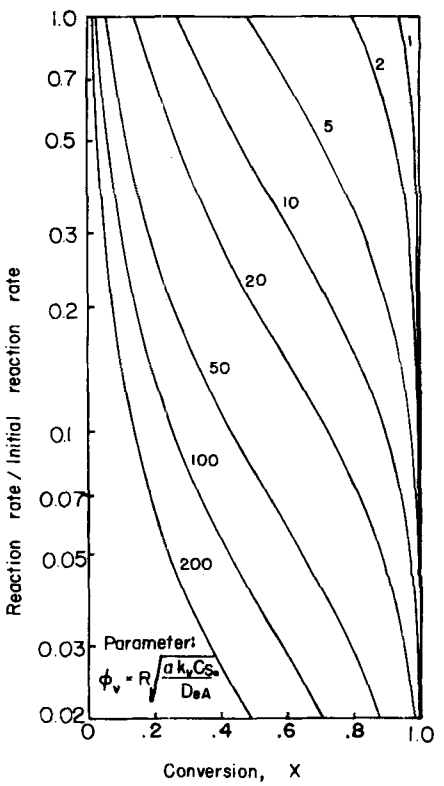

Fig. 6. Relation between conversion and reaction rate for $N_{Sh} = \infty$ and $D_{eA} = D'_{eA}$.

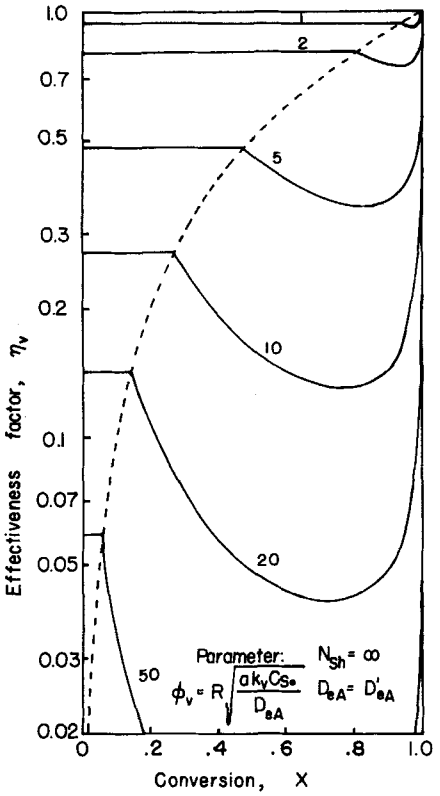

Fig. 7. Effect of ϕ_v on effectiveness factor.

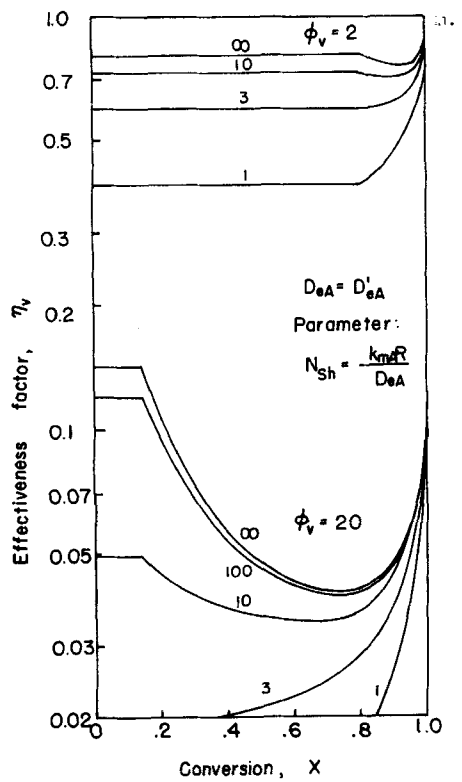

Fig. 8. Effect of N_{Sh} on effectiveness factor.

These results are exactly the same as those obtainable from the unreacted-core shrinking model under a pseudo steady state assumption when the ash diffusion is the rate-controlling factor. Therefore, when the diffusion through the solid is rate controlling, there is no way to distinguish from experimental data which of the two models is correct for the given system. Weisz and Goodwin (6) observed during the combustion of carbon deposited catalysts that at high temperature (625°C.) the carbon combustion is characterized by a shell progressive burn-off. At an intermediate temperature (515°C.), a transition existed which is characterized by a model between the homogeneous model and the unreacted-core shrinking model.

On the other hand, if the chemical reaction is very slow and is the rate controlling factor, ϕ_v approaches zero and

$$C'_A = C_{Ao} \quad \text{for} \quad 0 \leq r \leq R$$

$$\frac{C_S}{C_{So}} = 1 - \frac{\theta_v}{\theta_v^*}$$

$$X = \theta_v/\theta_v^* \quad \text{and} \quad \theta_v^* \propto R^0 \text{ (independent of } R).$$

As shown in Figure 5, the relation between X and θ_v/θ_v^* is not greatly different from that of the unreacted-core shrinking model, and therefore determination of a correct model from the experimental data is rather difficult.

For a clear demonstration of the difference between the two models, the rate of reaction is plotted against the solid reactant conversion as shown in Figure 6. In Figure 7, the relation between the effectiveness factor and the conversion obtained from Equations (33) and (35) is shown. As the values of ϕ_v are increased above 1, the effectiveness factor becomes smaller moving towards the diffusion controlled region. However, at complete conversion ($X = 1$), η_v becomes unity for all ϕ_v returning to the chemical reaction controlled region. In Figure 8, the effect of gas-film diffusion is shown for $\phi_v = 2$ and 20. As N_{Sh} becomes smaller than 100, the effect becomes apparent and is particularly significant during the first stage reaction.

THE UNREACTED-CORE SHRINKING MODEL ($D'_{eA} << D_{eA}$)

Next, we consider the case where D'_{eA} is very much smaller than D_{eA}. Under this condition ϕ'_v becomes large so that $\ln[\xi_m \sinh\phi'_v/\sinh(\phi'_v \xi_m)]$ can be approximated by $\phi'_v(1 - \xi_m)$. Also, since D'_{eA}/D_{eA} is small, Equations (28) and (31) become

$$\frac{\theta_v}{\phi'_v} = 1 - \xi_m + \frac{\phi_v}{2}\sqrt{\frac{D'_{eA}}{D_{eA}}}(1 - \xi_m^2) + \frac{\phi_v}{3}\sqrt{\frac{D'_{eA}}{D_{eA}}}\left(\frac{1}{N_{Sh}} - 1\right)(1 - \xi_m^3) \quad (35)$$

$$X = 1 - \xi_m^3 \quad (36)$$

These equations are equivalent to the equations derived based on the unreacted-core shrinking model under a pseudo steady state assumption:

$$\theta_S = 1 - \xi_c + \frac{\phi_S}{2}(1 - \xi_c^2) + \frac{\phi_S}{3}\left(\frac{1}{N_{Sh}} - 1\right)(1 - \xi_c^3) \quad (37)$$

$$X = 1 - \xi_c^3 \quad (38)$$

where

$$\phi_S = \frac{Rak_sC_{So}}{D_{eA}} \text{ and } \theta_S = \frac{k_s(C_{Ao} - C_A^*)\,t}{R}$$

Here $\xi_m (= r_m/R)$ is equivalent to $\xi_c (= r_c/R)$ for the unreacted-core shrinking model, and k_s is the reaction rate constant based on the reaction surface of the shrinking core.

The similarity of the two models when ϕ'_v is large can be realized from Figure 3 in which $(C'_A - C_A^*)$ becomes nearly zero in the reaction zone for ϕ'_v larger than 100, indicating no penetration of gas A into the shrinking core. Comparing Equations (35) and (36) with Equations (37) and (38), we can relate the surface-based quantities k_s, ϕ_s and θ_s to the volume-based quantities k_v, ϕ_v, and θ_v as

$$\phi_S = \phi_v \sqrt{\frac{D'_{eA}}{D_{eA}}}, \quad \theta_s = \theta_v/\phi'_v, \quad \text{and } k_s = \sqrt{\frac{D'_{eA}k_v}{aC_{So}}} \tag{39}$$

An example of the difficulties associated with the determination of a proper model for a solid-gas reaction system from experimental data can be shown for the case of the reduction of iron oxide with hydrogen. Most investigators used the unreacted-core shrinking model to analyze the rate-controlling factors and reported the activation energy as varying from 4.2 to 15 Kcal./g.-mole (2 to 5).

These values seem to be too small in comparison with most of the solid-gas reaction systems. Since the particles used in the experiments are mostly pelletized, D'_{eA} is not quite equal to zero although it is smaller than D_{eA}. In addition, the gradual transition of the various iron oxides (hematite → magnetite → wüstite) is taking place in zones within the pellet. This seems to indicate that the application of the unreacted-core shrinking model is unsuitable to this process. As shown in Equation (39), k_s is proportional to $\sqrt{k_v}$; therefore, the activation energy obtained based on the unreacted-core shrinking model could be as small as one-half of the true value. It was also pointed out in the previous section that the shapes of curves relating conversion and time are so similar for the various models (shown in Figure 5) that this criterion alone is not sufficient to determine the prevailing mechanism. It is hoped that the study presented here will be useful in the explanation of the abnormally low activation energies obtained in various experimental investigations.

CONCLUSION

An analytical solution under the pseudo steady state assumption is obtained for a model of solid-gas reactions taking place in a single particle. This model is represented by the first stage and the second stage reaction with the second stage being characterized by the diffusion through an ash layer and the reaction in an inner core. The effective diffusivities for the two zones D_{eA} and D'_{eA} are considered different but are constant during the course of reaction. The effectiveness factors are also defined for solid-gas reactions, and the effects of diffusion are examined. This model is shown to become the homogeneous model when $D_{eA} = D'_{eA}$ and the unreacted-core shrinking model when $D_{eA} >> D'_{eA}$. The two rate constants involved in the expressions of these models are related by

$$k_s = \sqrt{\frac{D'_{eA}k_v}{aC_{So}}}$$

It was also found that the unreacted-core shrinking model is valid for $\phi'_v > 100$. Some difficulties involved in selecting a proper model for analysis of experimental data are also discussed.

ACKNOWLEDGMENT

This work was supported by grants from the Public Health Service and the National Aeronautics and Space Administration. The authors wish to thank Takashi Shirai, Eizo Sada, and S. C. Wang for their help in discussions of this paper.

NOTATION

a = stoichiometric coefficient
C_A = concentration of component A in gas, C'_A in reaction zone, C_{Ao} in bulk phase, C_{Am} at boundary between reaction zone and ash layer, C_{As} at outer surface of particle, moles/L^3
C_A^* = equilibrium concentration of component A, moles/L^3
C_S = concentration of solid reactant S, moles/L^3
C_{So} = initial concentration of solid reactant, moles/L^3
D_{eA} = effective diffusivity of component A in ash layer, L^2/θ
D'_{eA} = effective diffusivity of component A in reaction zone, L^2/θ
k_{mA} = mass transfer coefficient, L/θ
k_s = reaction rate constant based on area, L^4/(moles θ)
k_v = reaction rate constant based on volume, L^3/(moles θ)
M_A = total reaction rate of component A, mole/θ
M_S = total reaction rate of component S, mole/θ
N_{Sh} = $k_{mA}R/D_{eA}$
N'_{Sh} = $k_{mA}R/D'_{eA}$
R = particle radius, L
r = distance from the center of sphere, L
r_A = reaction rate for gas component A, moles/$(L^3 \cdot \theta)$
r_S = reaction rate for solid reactant S, moles/$(L^3 \cdot \theta)$
r_m = r at boundary between reaction zone and ash layer, L
r_c = distance from the center of sphere to unreacted core surface, L
t = time, θ
t^* = time for complete conversion, t_c time for completion of first stage reaction, θ
V = volume, L^3
X = conversion

Greek Letters

η_v = effectiveness factor
θ_v = dimensionless time, θ_{vc} for complete reaction of the first stage, θ_v^* for complete reaction of both stages
ξ = dimensionless radius, $\xi = r/R$, $\xi_m = r_m/R$
ϕ_v = Thiele modulus based on D_{eA}, ϕ'_v based on D'_{eA}
ϵ = voidage of particle

LITERATURE CITED

1. Ausman, J. M., and C. C. Watson, *Chem. Eng. Sci.*, **17**, 323 (1962).
2. Feinman, Jerome, and T. D. Drexler, *AIChE J.*, **7**, 584 (1961).
3. McKewan, W. M., *Trans. Am. Inst. Mech. Engrs.*, **218**, 2 (1960).
4. *Ibid.*, **221**, 140 (1961).
5. Themelis, N. J., and W. H. Gauvin, *ibid.*, **227**, 290 (1963).
6. Weisz, P. B., and R. D. Goodwin, *J. Catalysis*, **2**, 397 (1963).
7. Yagi, S., and D. Kunii, "Fifth Symposium (International) on Combustion," p. 231, Reinhold, New York (1955).

Manuscript received May 3, 1967; revision received September 26, 1967; paper accepted September 27, 1967.